BOREAL ENVIRONMENT RESEARCH 25: 51–63
ISSN 1797-2469 (online)

Helsinki 24 April 2020

Estimation of the maximum and minimum surge levels at the Hanhikivi peninsula, Gulf of Bothnia

Svetlana M. Gordeeva[1)3)†*] and Konstantin A. Klevannyy[2)]

[1)] *Russian State Hydrometeorological University, 79, Voronezhskaya St., St. Petersburg, 192007, Russia (*corresponding author's e-mail: gordeeva@rshu.ru)*
[2)] *CARDINAL LLC, Office 19, 77/3, Severnyy Pr., St. Petersburg, 195256, Russia*
[3)] *Shirshov Institute of Oceanology, Russian Academy of Sciences, 36, Nahimovskiy Pr., Moscow, 117997, Russia*
[†] *Present address*

Received 13 Aug. 2019, final version received 19 Mar. 2020, accepted 25 Feb. 2020

Gordeeva S.M. & Klevannyy K.A. 2020: Estimation of the maximum and minimum surge levels at the Hanhikivi peninsula, Gulf of Bothnia. *Boreal Env. Res.* 25: 51–63.

A combination of statistical and deterministic methods was used to calculate the flood level for the Hanhikivi peninsula on the northeastern coast of the Gulf of Bothnia, where a nuclear power plant is planned. An existing Baltic Sea numerical model (BSM-2010) solving the depth-averaged shallow water equations was used. Using formulas for an idealized storm field, wind and atmospheric pressure fields were assigned as forcing. The possible intensity of the extreme storm field was determined from the database of storm fields that passed over the northern hemisphere from 1958–2016. The modeling results show that the maximum water level rise at Hanhikivi occurs when an extreme storm field over southern Norway moves east-northeast with a velocity of 65 km h^{-1}. Extreme water levels in Hanhikivi obtained with statistical and deterministic methods at a probability up to 0.01% (return period of 10^4 years) are +252 cm and –251 cm, respectively.

Introduction

The construction of a nuclear power plant is being designed on the Hanhikivi cape in the Pyhäjoki municipality on the northeastern coast of the Gulf of Bothnia, Finland (Fig. 1, 64.5°N, 24.3°E). For this, one needs to know the extreme hydrodynamic conditions of this region. These characteristics include, among others (Helander 2017), the maximum and minimum water levels with an annual exceedance probability of up to 0.01% (once in 10^4 years) (International Atomic Energy Agency 2011).

Tides do not play an important role in Baltic Sea flow dynamics (Leppäranta and Myrberg 2009). Surges on the coast of the Gulf of Bothnia are caused by the passage of low pressure storm fields over the water and are accompanied by wind waves, which increase the storm surge level.

Fall and winter are the windiest seasons. The most common wind directions are from the south and southwest, whereas the wind direction from the northwest is the most improbable. The mean wind speed reported at the closest weather station (Raahe Lapaluoto) to Hanhikivi is 5.9 m s^{-1}. In November, it increases to 6.9 m s^{-1}. The maximum wind speed with an occurrence up to 0.01% in Raahe Lapaluoto is 29 m s^{-1} and in Raahe Nahkiainen, an off-

Editor in charge of this article: Kai Myrberg

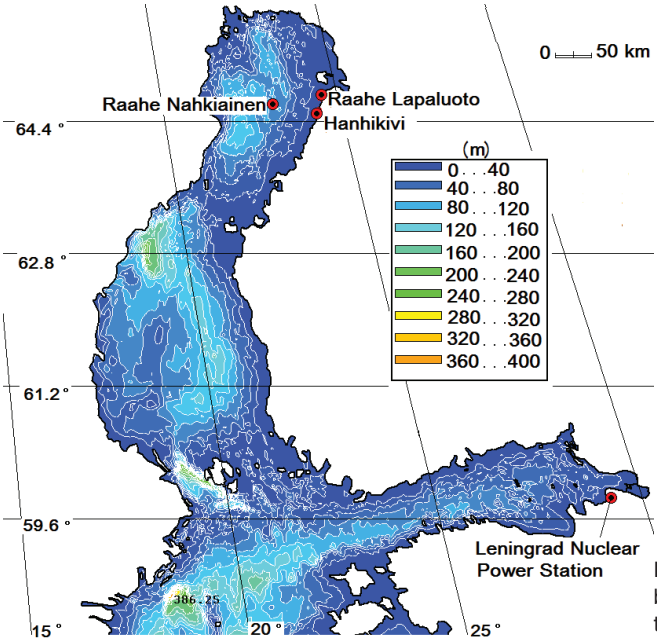

Fig 1. The location of the study area and the bathymetric model of the Gulf of Bothnia and the Gulf of Finland.

shore weather station, is 33.8 m s^{-1} (Laapas M., Hyvärinen A. & Mäkelä A., unpublished). In recent decades, while the total number of storm fields over the North Atlantic is decreasing, the proportion and number of storm fields with a wind speed of more than 25 m s^{-1} have been constantly increasing, which indicates an increase of storm activity in the Baltic (Vyazilova and Vyazilova 2014, Wolski 2014). Furthermore, a shift of the trajectories of the low pressures to the north is observed (Vyazilova and Vyazilova 2014). When storm event "Erwin", which is the strongest of the last 20–40 years (Suursaar *et al.* 2006, Soomere *et al.* 2008), passed across the Baltic Sea on 8–9 January 2005, many observation stations in the Gulf of Finland and beyond reported that the historic water level maxima were exceeded.

At Raahe, the maximum water level recorded is 162 cm, which occurred on 14 January 1984 (Finnish Meteorological Institute, unpublished). According to the recommendations of the International Atomic Energy Agency for determination of design levels, the extreme water level rise must be computed using both statistical and deterministic modeling methods (IAEA 2011). Modeling allows to determine which meteorological conditions can result in an extreme level obtained by statistical methods and to estimate its probability from a meteorological point of view.

In Averkiev and Klevannyy (2009, 2010), Apukhtin *et al.* (2017), the maximum possible surge level was simulated for the area of the Leningrad nuclear power plant, located on the coast of Koporskaya Bay of the Gulf of Finland. They reported that the maximum water level rise will occur when an extreme storm field propagates with a sufficiently high velocity along a trajectory crossing the south of Finland and the pressure deep is at its maximum when the cold front passes over Koporskaya Bay.

In the present study, we determined the parameters of the extreme storm field, which has a rare frequency on the northeast coast of the Gulf of Bothnia and simulated the sea level fluctuation during the passage of such a storm field along different trajectories of the pressure deep at different velocities. After determining the most dangerous trajectory for the Hanhikivi peninsula and the associated water level rise or fall, the probability of such an event was estimated using the database (Serreze 2016), which holds the information on storm fields of the northern hemisphere, from 1958–2016. The study of the impact of moving low pressure atmospheric sys-

tems on water level in the Hanhikivi area has not been previously investigated.

Material and methods

Description of the modeling system

The simulations were performed with the CARDINAL software package (Klevannyy *et al.* 1994, Klevannyy and Smirnova 2009; available at http://cardinal-hydrosoft.ru) using the Baltic Sea model, BSM-2010. In general, CARDINAL solves the three-dimensional baroclinic equations and BSM-2010 uses two-dimensional shallow water equations.

The 2D shallow water equations may be written in the following form (see e.g., Leppäranta and Myrberg 2009):

$$\boldsymbol{U}_t + \frac{(\boldsymbol{U}\nabla)\boldsymbol{U}}{H} = -gH\nabla\varsigma - \frac{H\nabla P_a}{\rho_0} + \boldsymbol{f}\times\boldsymbol{U} + K\Delta\boldsymbol{U} + \frac{\tau}{\rho_0} - \frac{f_b\boldsymbol{U}|\boldsymbol{U}|}{H^2}, \quad (1)$$

$$\zeta_t + \mathrm{div}\boldsymbol{U} = 0, \quad (2)$$

where $\boldsymbol{U}$ is the vector of specific horizontal water flow (full flow), $H = h + \zeta$ is the water depth, h is water depth from the zero level (which is counted vertically downwards), ζ is the free surface level (which is counted from the zero level and vertically upwards), g is the gravitational acceleration, ρ_0 is the water density, P_a is the atmospheric pressure, f is the Coriolis parameter, K is the horizontal eddy viscosity coefficient, τ is the shear wind stress and f_b is the bottom friction coefficient.

At the solid boundaries the normal component of velocity was set to zero and the tangential one was determined from the slip condition. The horizontal eddy viscosity coefficient, K, was determined with the "4/3" law (Okubo and Ozmidov 1970). For extreme winds, the accuracy of the results crucially depends on the specification of the shear wind stress: when the wind velocity is more than 30 m s^{-1}, the wind drag coefficient decreases (Jarosz *et al.* 2007). The model calculations use the procedure for calculating tangential stress according to Makin (2005). This requires data on the parameters of wind waves, which were obtained for example, from the SWAN model (http://www.swan.tudelft.nl). The equations were solved by finite-difference methods on a curvilinear boundary-fitted grid generated by the Thompson elliptic method (Thompson *et al.* 1985). A procedure for drying and flooding the cells of the computational grid was included.

The BSM-2010 model grid consists of 300 321 nodes (681×441) and covers an area of 387 607 km^2 with a still water volume of 20 891 km^3. The digitized coastline was obtained from the NOAA database (http://www.ngdc.noaa.gov/mgg/dat/geodas/coastlines/LittleEndian/coast41.zip). The western boundary of the computational area was defined at the narrowest part of the Danish straits. The depth field was derived mainly from data navigation maps of the Baltic Sea region countries and was obtained during the implementation of the HIROMB project. At station Hanhikivi, the still water depth in the model was 3.7 m and at Raahe it was 3.4 m. The average water depth in the model was 53.8 m and the maximum was 371 m. The average distance between the water level grid points was 3.6 km and the maximum and minimum distances were 19.1 km (far from the area of interest) and 110 m, respectively. The bottom friction coefficient f_b was set to equal 0.0026.

Since December 1999, the Baltic Sea models developed with the CARDINAL are operationally used at the Northwest Hydrometeorological Service of Russia to forecast water levels and warn of the threat of floods in St. Petersburg. Atmospheric forcing results from the HIRLAM model of SMHI (Norrköping, Sweden) were used. Discharges through the Danish straits were prescribed used forecasts made by BSH (Hamburg, Germany). From December 2007, HIRLAM forecast data are received two times per day, and from April 2008, four times per day. Table 1 shows the forecast accuracy for St. Petersburg and its improvement over time (Klevannyy and Mostamandy 2009). Clearly, refreshing the meteorological forecast every six hours has significantly improved the model forecasts. An example of observed and simulated HIRLAM 24 hour forecasts time histories of the water level in Raahe for January 2007 is shown

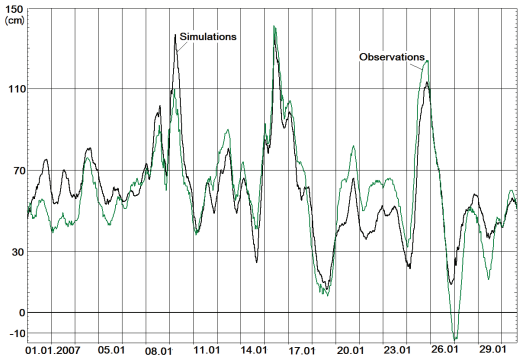

Fig 2. Observed (green) and BSM-2010-simulated with 24 hours HIRLAM forecasts (black) of the water level history in Raahe of the month of Jan. 2007.

in Fig. 2. On 16 January 2007, the recorded water level was 141 cm. Statistics of this forecast is rather good: the spread is 13 cm, the mean absolute error is 10 cm and the correlation coefficient is 0.87.

The basis of the pressure field for the idealized storm field uses the parameterization proposed in Miyazaki *et al.* (1962); the wind field was then calculated according to Sorkina (1958). Isobars in Miyazaki *et al.* (1962) were considered circular. For storm fields, this does not contradict observational data.

In Averkiev and Klevannyy (2009, 2010) the strengthening of the wind on the cold front of the storm field and the temporal evolution of pressure at its center were taken into account. In this paper, the following additional changes were made to the description of the pressure and wind fields: 1) the distance from the center of the storm field (i.e., location of the minimum pressure) was determined, taking into account the Earth's curvature along a large circle arc; 2) the formula describing the time evolution of pressure at the center of the storm field was changed; and 3) the inclination angle of the wind relative to the isobars according to Bretschneider (1972) was made dependent on the distance to the center of the storm field (it now increases with a distance from 10° to 25°).

Pressure and wind fields were calculated with the formulas:

$$P_a(x,y,t) = P_\infty - \frac{\Delta P_o \exp\left(-\left[\frac{t-T_0}{\Delta T}\right]^2\right)}{\sqrt{1+\left(\frac{r}{r_T}\right)^2}} \left[1-\gamma_1 \exp\left(-\frac{|\boldsymbol{r}|-r_T}{r_T}\right)\exp\left(-\gamma_2\frac{|\alpha-\alpha_0|}{\alpha_2-\alpha_1}\right)\right], \quad (3)$$

$$W_x = -\frac{0.6}{\rho_a f}\left[\frac{\partial P_a}{\partial y}\cos\beta + \frac{\partial P_a}{\partial x}\sin\beta\right], \quad (4)$$

$$W_y = \frac{0.6}{\rho_a f}\left[\frac{\partial P_a}{\partial x}\cos\beta - \frac{\partial P_a}{\partial y}\sin\beta\right], \quad (5)$$

where r is the distance from the centre of the storm field $x_c(t)$, $y_c(t)$ to the point (x, y), r_T is the radius of maximum wind, ΔP_0 is the difference between the pressure outside the storm field, $P\infty$, and the pressure at the center of the moment, T_0, when the pressure drop is at the greatest, ΔT is the parameter that determines the duration of the storm field existence (from

Table 1. Statistical assessment of the St. Petersburg water level forecasts made with the BSM-2010 modeling system with the CARDINAL software for different years.

Year	Spread (cm)	Bias (cm)	Mean absolute error (cm)	Root mean simulated error (cm)	Correlation coefficient
2000	19	4	15	19	0.76
2002	16	–8	13	18	0.79
2003	16	–6	13	18	0.78
2004	14	3	12	14	0.87
2005	15	4	11	15	0.89
2006	16	2	11	16	0.90
2007	17	1	12	17	0.86
2008	11	0	8	11	0.93
2009	10	1	7	10	0.94

time $t = T_0 \pm \Delta T$ to $t = T_0$, the pressure difference at the center of the storm field and outside it will increase from 0.37 ΔP_0 to ΔP_0), α_1, α_2 , γ_1 and γ_2 are coefficients that take into account the strengthening of the wind on a cold front, located southwest from the center of the cyclone $x_c > x$, $y_c > y$, $\alpha_0 = (\alpha_1+\alpha_2) / 2$, $\alpha = \text{arctg}[(x_c - x)/(y_c - y)]$ and ρ_a is the air density.

It may be shown (see e.g., Averkiev and Klevannyy 2010) that at the distance $r = r_T$ (Eq. 3) gives the maximum wind velocity (excluding the front).

The distance r was determined with the formula:

$$r = R \arccos[\sin\varphi_c \sin\varphi + \cos\varphi_c \cos\varphi \cos(\lambda_c - \lambda)], \quad (6)$$

where (φ_c, λ_c) and (φ, λ) are the latitude and longitude at the center of the storm field (x_c, y_c) and point (x, y), respectively and R is the Earth's radius.

The wind inclination angle, β, relative to isobars follows the formula proposed in Bretschneider (1972):

$$\beta = \begin{cases} 10^\circ(1+\frac{r}{r_T}), & 0 \le r < r_T \\ 20^\circ + 25^\circ(\frac{r}{r_T} - 1), & r_T \le r < 1.2r_T \\ 25^\circ, & r \ge 1.2r_T \end{cases}. \quad (7)$$

An estimate of ΔT was obtained from the analysis of the synoptic situations of the eight strongest storm fields that passed over the Baltic Sea from 1967–2005 (Apukhtin *et al.* 2017). The range of ΔT found was from 36–60 hours. It was shown in Averkiev and Klevannyy (2009) that an increase in ΔT leads to an asymptotic increase in the simulated water level rise. In the calculations presented below, $\Delta T = 50$ hours was used.

The following values of the coefficients in expression (Eq. 3) are obtained from the analysis of weather charts: $\gamma_1 = 0.003$ if $x_c > x$ and $y_c > y$, otherwise $\gamma_1 = 0$, $\gamma_2 = 3.0$, $\alpha_1 = \pi r / (18 r_T)$; $\alpha_2 = \alpha_1 + 2\pi / 9$, $P\infty = 101\,000$ Pa; $\Delta P_0 = 5\,000$ Pa.

Statistical analysis of sea level changes

Following the recommendations of the International Atomic Energy Agency (IAEA), the calculation of the probabilities of annual maximum and minimum levels (measured relative to the mean level) and their extrapolation to the area of low probabilities were carried out by applying the Gumbel distribution (Sikan 2007, Johnson *et al.* 1995). Calculations of the probability of exceedance, P, were performed using:

$$z(P) = M - \frac{1}{\theta}\ln(-\ln(1-P)), \quad (8)$$

where $M = \bar{z} - 0.45\sqrt{\sigma^2}$, $\theta = 1.28 / (\sqrt{\sigma^2})$, $\bar{z}$ is the mean annual extreme level and σ^2 is the variance.

Additionally, to clarify the type of probability distribution for the extreme cases, we used the program CumFreq (Oosterbaan 2019, available at: https://www.waterlog.info/cumfreq.htm) and calculated the parameters of 16 probability distributions.

Data

We used the average annual sea level in Raahe according to the Permanent Service for Mean Sea Level database (https://www.psmsl.org/data/obtaining/stations/240.php) as well as the characteristics of its annual extremes relative to mean sea level (Finnish Meteorological Institute data, unpublished).

Raahe is located closer to the top of the Gulf of Bothnia than Hanhikivi, therefore the surge peaks at Raahe should be greater. Since there were no hydrological observations at Hanhikivi station, we used modeling results to correlate sea level estimates at the stations.

Hydrodynamic modeling of various extreme situations give simultaneous values of the maximum and minimum sea levels in Raahe and Hanhikivi, which made it possible to find the linear regression transfer functions and get sea level assessments for Hanhikivi.

The following regression equations were obtained that expressed the statistical relationship of the maximum and minimum surge levels (in cm) at Hanhikivi and Raahe:

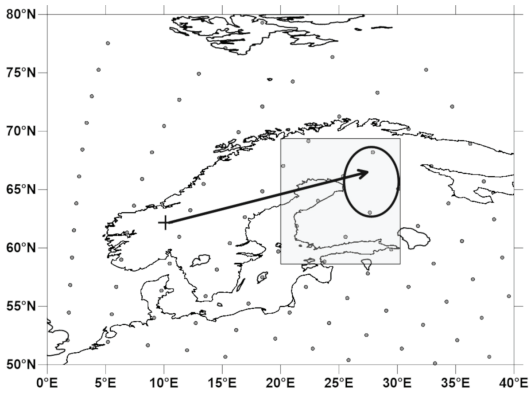

Fig 3. Study area for the storm field statistical analysis (gray rectangle). The black arrow indicates the most dangerous storm field trajectory for Hanhikivi, based on the model results. Black dots show the storm field reanalysis data grid, the oval indicates the area for examination of the relevant storm field characteristics.

$$Z^{+}_{Hanhikivi} = 0.95\ Z^{+}_{Raahe} + 3.39, \quad (9)$$

$$Z^{-}_{Hanhikivi} = 0.73\ Z^{-}_{Raahe} + 3.30. \quad (10)$$

Eq. 9 determines 98% of the variance of the series obtained and has a standard error of 5 cm. Eq. 10 also determines 98% of the variance of the series obtained and has a standard error of 7.2 cm (Table 2).

For the analysis of the characteristics of storm fields over the northern part of the Baltic Sea, the northern hemisphere cyclones from the 1958–2016 database (Serreze 2016), based on the NCEP/NCAR reanalysis was used. This archive includes 6 hour data for the following characteristics of extra tropical storm fields: (1) center position and pressure at the center of each storm field; (2) distance traveled by the storm field in the last 6 hours; (3) information on cyclogenesis and cyclolysis; (4) local Laplacian of pressure and; (5) barometric trend at the center of the storm field.

An area limited to latitudes of 59–70°N and longitudes 20–30°E was chosen for the analysis of trajectories of storm fields over the northern part of the European territory (gray rectangle in Fig. 3). For the period from 1958–2016, the database contains 2334 storm fields in this region. For all these storm fields coming to a given area, their paths from the moment of origin were determined.

Results and Discussion

Sea level changes at the Hanhikivi peninsula

Water level measurements at Raahe station, which is located 20 km north and it is nearest to station Hanhikivi, has been operating since 1922. Table 2 presents the statistical characteristics of the average annual sea level in Raahe according to the Permanent Service for Mean Sea Level database (PSMSL 2019) as well as the characteristics of its annual extremes relative to mean sea level from the FMI database. The annual sea level in Raahe has a significant negative trend due to the post-glacial uplift of the Fennoscandinavian plate. The continuing global mean sea level rise

Table 2. Statistics of annual mean, annual maximum and annual minimum sea level (cm) at Raahe and Hanhikivi stations.

Statistical characteristics	Annual mean	Raahe		Hanhikivi	
		Annual max. relative to annual mean	Annual min. relative to annual mean	Annual max. relative to annual mean	Annual min. relative to annual mean
Mean, x, cm	—	103.30	–80.27	101.29	–55.56
Std. Dev., σ, cm	20.24	23.66	17.89	22.42	13.12
Variation coeff., $C_v=\sigma/x$	0.03	0.22	–0.24	0.22	–0.24
Skewness, C_s	–0.03	–0.05	–0.53	–0.05	–0.53
Relation C_s/C_v	–1.13	–0.24	2.23	–0.24	2.23
Trend, cm/y^{-1} and (R^2)	–0.68 (0.87)	0.29 (0.10)	0.18 (0.07)	0.27 (0.10)	0.13 (0.07)

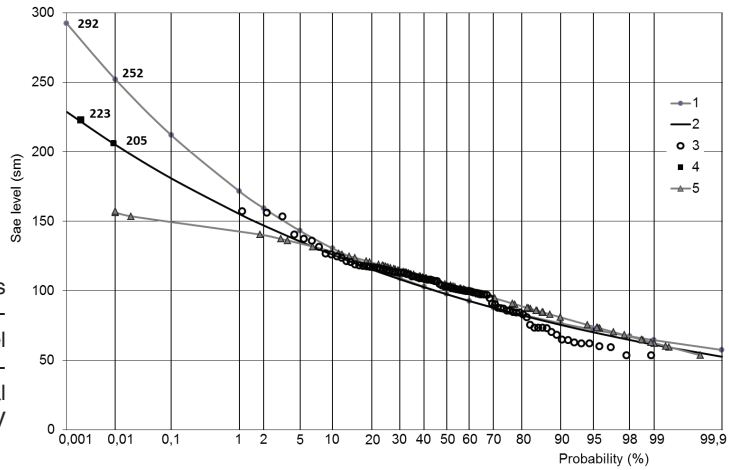

Fig 4. Probability exceedance curves of annual maximum levels in Hanhikivi, obtained using the (**1**) Gumbel statistical function and (**2**) deterministic methods. Included are (**3**) empirical and (**4**) model data points. (**5**) GEV statistical function is shown.

is 3.3 mm year^{-1} (University of Colorado; http://sealevel.colorado.edu) is reflected on the Baltic Sea mean water level and partially compensates post-glacial uplift. From 1923–2013, the observed decrease of mean water level in Raahe was –6.8 mm year^{-1}. The trend of the sea level maximum relative to the average sea level in Raahe was 2.9 mm year^{-1} and was small relative to its total variance. Johansson *et al.* (2001) estimated the same trend in Raahe to be 1.9 mm year^{-1}. Considering that their observation period was much shorter (1923–1999), we can conclude that the growth of the maxima in recent years has accelerated. A similar conclusion was made by Barbosa (2008) based on her calculation of sea level trends of small quantiles. In this case, for the maximum sea level values, the decreasing trend of average values is additionally compensated by their own trend, so it became –3.9 mm year^{-1}. Thus, the acceleration of climatic changes affecting the rise in the Baltic Sea can offset the continued rise of the Fennoscandinavian plate.

At Hanhikivi, the annual maximum values, on average, exceeded the annual mean sea level by 1 m, and the annual minimum values were below the annual mean level by 55 cm (Table 2). The temporal variability of the extreme characteristics showed positive trends that partially compensated the level decrease. So, the extreme intra-annual water level increase will change a little, while extreme decrease will be more pronounced.

The extreme sea level values were approximated by several different statistical methods. Fig. 4 shows the GEV and the Gumbel functions. Despite the best approximation of empirical data by the GEV function (error 4% versus 6% with the Gumbel function), it is obvious that it significantly underestimates the probability of positive extremes. Therefore, a further estimation of extreme values was done with the Gumbel function.

In Table 3, we present the estimates of extreme values of sea level in Raahe and Han-

Table 3. Extremes of sea level (cm, relative to the mean sea level) at Raahe and Hanhikivi with low probabilities, obtained with the Gumbel distribution.

Probability (%)	Water level at Raahe		Water level at Hanhikivi	
	Maximum	Minimum	Maximum	Minimum
1	177	–136	172	–97
0.1	220	–169	212	–120
0.01	263	–201	252	–144
0.001	305	–233	293	–168

hikivi, obtained with the Gumbel distribution. We see that the annual maximum level in Raahe with exceedance probabilities of 0.01% and 0.001% is +263 cm and +305 cm, respectively. The minimum level in Raahe with a probability of 0.01% is –201 cm and –233 cm for 0.001%.

At Hanhikivi, the obtained maximum level with exceedance probabilities of 0.01% and 0.001% is +252 cm and +293 cm, respectively. For the minimum level at Hanhikivi, these probabilities are –144 cm and –168 cm for 0.01% and 0.001%, respectively.

According to German and Levikov (1988) and Blackman and Graff (1978), the repeat period to which an observed probability curve can be extrapolated is roughly equal to four times the length of the observation series. With the available number of data years for Raahe is 92 years, this means that the curve cannot be extrapolated beyond a repeat period of 368 years, which is an annual exceedance probability of 0.3%. Note that the Gumbel method at the exceedance probability of 1% gave a noticeable difference compared with extrapolation of the observations at Raahe are 177 cm and 162 cm, respectively.

Determination of the relevant extreme storm field

A characteristic of the intensity of the storm fields is the Laplacian of pressure at its center at the moment of maximum deepening where the estimated value depends on the distance between the points where the pressure was measured (Kouroutzoglou *et al.* 2011).

It was shown that of the 2334 cyclones registered over northwestern Europe, the maximum value of the Laplacian of pressure equals 47.75 mPa km^{-2}. This value was observed on 25 October 1985 in northern Norway. The value of 59 mPa km^{-2} corresponds to a repeat time of 1000 years (Apukhtin *et al.* 2011).

For the model storm field (Eq. 3), this maximum value of the Laplacian was obtained with 6 hour averaging and 250 km spatial resolution of the grid (for r_T = 250 km). The values of pressure and wind speed for the numerical simulations were computed on a rectangular 10 km grid for the whole specified period with the time step of 1 hour. Hourly values of the Laplacian of pressure for the period of ±3 hours to the maximum computed from Eq. 3 for ΔT = 50 hours were equal to 33, 57, 78, 91, 74, 51 and 28 mPa km^{-2} respectively.

We determined the most dangerous trajectory and velocity of the storm field, leading to maximum water rise at Hanhikivi by a series of experiments, by successively varying one of four parameters in each experiment series. These parameters are: 1) latitude of the initial location of cyclone center, φ_1; 2) location λ_2; and 3) location φ_2 of the cyclone center at the moment T_0 of minimal pressure for the whole period (MP); and 4) the velocity vector $\boldsymbol{V}_c$ of the storm field center. The initial longitude, λ_1, was set at a constant 10°E and at a sufficient distance from Hanhikivi. Therefore, we consider that only storm fields coming from the west corresponds to the real situation. According to Serreze (2016), only one storm field with Laplacian of pressure above 30 mPa km^{-2} came from the east over the Baltic Sea region. For each calculation, the assigned values of these five parameters were used to calculate those present in the formulas for the pressure field, the zonal V and the meridional U components of the storm field velocity and the time T_0 required to move it along the arc of the large circle from the starting point to the final one. The calculation of pressure and wind is performed for the entire specified calculation period.

In the experiments with varying φ_2, the storm field moves along various parallels strictly eastward with a velocity of 75 km h^{-1} with MP on 27°E. It was found that the level maximum at Hanhikivi in this case occurs for φ_2 = 66.1 — i.e., the center of the storm field moves along the 66.1°N parallel (Table 4). For storm fields moving along φ_2 = 66.1°N, we change λ_2. The maximum water level at Hanhikivi is obtained for λ_2 = 27°E. We then set λ_2 = 27°E, and φ_2 = 66.1°N and move the storm field to this point starting from different values of φ_1. We obtain the maximum level for φ_1 = 61.6°N. Now, with the fixed storm field trajectory (along a large arc circle from λ_1 = 10°E, φ_1 = 61.6°N to λ_2 = 27°E, φ_2 = 66.1°N) we change its velocity. We found that the velocity dependence is nonmonotonic.

The maximum sea level rise was obtained for V_c = 65 km h^{-1}. In the next series of experiments φ_2 was varied with fixed φ_1 = 61.6°N, λ_2 = 27°E, V_c = 65 km h^{-1}. The maximum sea level rise was found for φ_2 = 66.2°N. Then, in the second approximation we changed λ_2 for a storm field moving with V_c = 65 km h^{-1} from λ_1 = 10°E, φ_1 = 61.6°N to φ_1 = 66.2°N. The maximum level rise was again obtained for λ_2 = 27°E. In the last series of experiments, we varied φ_1 with fixed φ_2 = 66.2°N, λ_2 = 27°E, V_c = 65 km h^{-1}. We found that the maximum level was insensitive to the variation of φ_1 and therefore the calculations were not resumed.

The maximum rise of +223 cm at Hanhikivi is obtained for the storm field moving from φ_1 = 61.6°N, λ_1 = 10°E to MP at φ_2 = 66.2°N, λ_2 = 27°E with a velocity of 65 km h^{-1} (Figs. 5–7). Maximum wind speed was 39 m s^{-1}.

The maximum level in Hanhikivi equaled to 205 cm for 0.01% probability (47 cm lower than that obtained with the statistical method), the minimum level found was –251 cm (107 cm lower than that obtained with the statistical method) (Fig. 4).

Determination of the wind wave data

At the moment of maximum water rise in Hanhikivi, we calculated wind waves using SWAN. The calculation was performed in a stationary mode on the BSM-2010 model grid. The input parameters were wind and depth and the water level and water current results were exported from the BSM-2010 flow model. The output parameters of the SWAN calculations are the fields of significant wave heights (h_s), the average wave periods and the maximum orbital velocity at the bottom. The simulated wave height in the Gulf of Bothnia reaches 9 m SW of Hanhikivi (Fig. 8). As it approaches the shore, the wave height decreases to 2.5 m. The relevant periods of wind waves reach 10 s, decreasing in the region of Hanhikivi to 5 s. The near-bottom orbital velocity in waves near the coast of Hanhikivi reaches 60–70 cm s^{-1}.

Mathematical modeling of storm surge sea levels in Hanhikivi area

Using database of the northern hemisphere cyclones from 1958–2016, we first determined which storm field trajectories intersect the 10°E meridian in the latitudinal zone 60–62°N (297 cases). Of these, we selected those that come to the area of maximum deepening (50 cases; see oval in Fig. 3). Next, we determined the average velocity of movement of these storm fields over northwestern Europe (Fig. 9). For the period from 1958–2016, the average velocity of these storm fields was 39.4 km h^{-1}. In recent years (Fig. 9), the number of storm fields with the most dangerous trajectory has increased 1.5 times: in the 32 years from 1958–1990, 22 cyclones; and in the 27 years from 1990–2016, 28 cyclones. However, the trend towards an increase of the average velocity of about 0.8 km h^{-1} per decade shown on Fig. 9 is insignificant.

Table 4. Numerical experiments with trajectories and velocities of low pressure system aimed to find the maximum water level rise in Hanhikivi.

Fixed parameters	Max. level in Hanhikivi is found for:	Max. level in Hanhikivi (cm)
λ_1 = 10°E, λ_2 = 27°E, V_c = 75 km h^{-1}	$\phi_1 = \phi_2$ = 66.1°N	166
λ_1 = 10°E, $\phi_1 = \phi_2$ = 66.1°N, V_c = 75 km h^{-1}	λ_2 = 27°E	166
λ_1 = 10°E, λ_2 = 27°E, ϕ_2 = 66.1°N, V_c = 75 km h^{-1}	ϕ_1 = 61.6°N	218
λ_1 = 10°E, ϕ_1 = 61.6°N, λ_2 = 27°E, ϕ_2 = 66.1°N	V_c = 65 km h^{-1}	222
λ_1 = 10°E, ϕ_1 = 61.6°N, λ_2 = 27°E, V_c = 65 km h^{-1}	ϕ_2 = 66.2°N	223
λ_1 = 10°E, ϕ_1 = 61.6°N, ϕ_2 = 66.2°N, V_c = 65 km h^{-1}	λ_2 = 27°E	223
λ_1 = 10°E, ϕ_2 = 66.2°N, λ_2 = 27°E, V_c = 65 km h^{-1}	ϕ_1 = 61.6°N	223

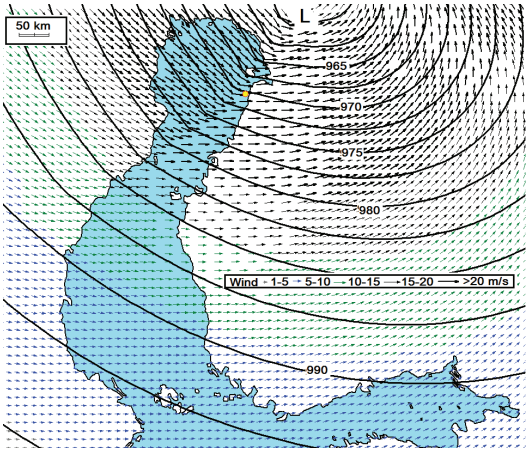

Fig 5. Wind and pressure fields over the Gulf of Bothnia and the Gulf of Finland for an idealized storm field moving along the most dangerous trajectory at the moment of the maximum level rise in Hanhikivi. The storm field moved from 61.6°N, 10°E to MP position at 66.2°N, 27°E with a velocity of 65 km h^{-1}. The maximum water level rise in Hanhikivi is +223 cm.

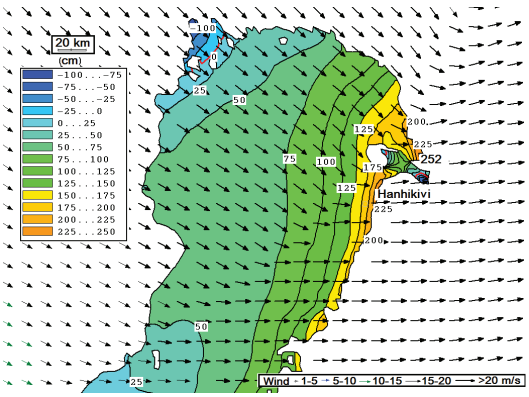

Fig 6. Water level isolines (cm) and wind vectors in the northern part of the Gulf of Bothnia at the moment of the maximum water level rise at Hanhikivi. All parameters are the same as in Fig. 5. The maximum water level rise in Hanhikivi is +223 cm.

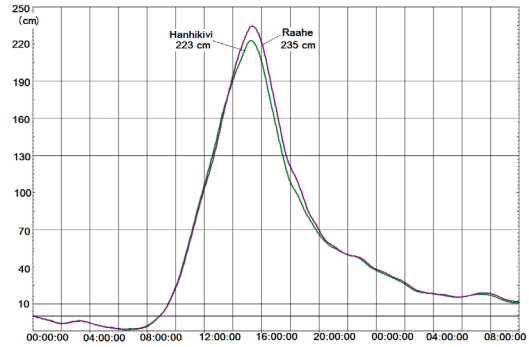

Fig 7. Time history of water level for Hanhikivi and Raahe during the passage of an extreme storm field along the most dangerous trajectory from position 10°E, 61.6°N to MP position at 66.2°N, 27°E, with a velocity of 65 km h^{-1}.

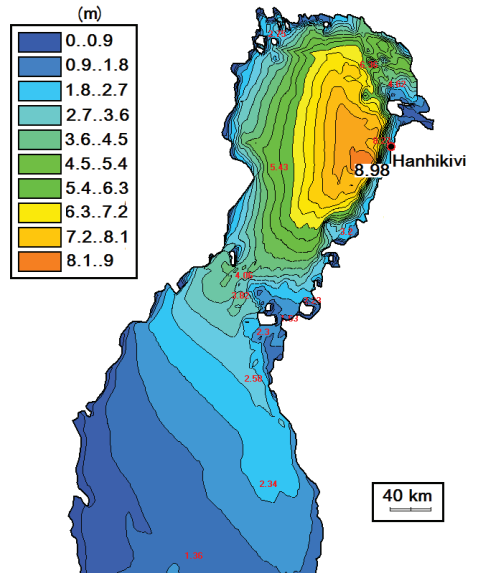

Fig 8. Isolines of significant wave heights (hs) in the northern part of the Gulf of Bothnia at the moment of the maximum water level in Hanhikivi during the passage of an extreme storm field along the most dangerous trajectory.

Table 5. Storm fields with average velocity of more than 60 km h^{-1} over northwestern Europe and moving along the most dangerous trajectory.

Date and Time	Avg. velocity (km h^{-1})	Max. velocity (km h^{-1})	Coordinates of max. velocity	Coordinates of max. pressure deepening
13–14 Dec. 1964	60.3	84.6	68.19°N, 27.90°E	60.41°N, 15.64°E
8 Jan. 1994	63.0	92.9	68.19°N, 27.90°E	62.64°N, 16.93°E
23 Sep. 2003	64.6	93.0	68.19°N, 27.90°E	68.19°N, 27.90°E
9–10 Jan. 2007	62.4	91.1	63.23°N, 12.36°E	63.23°N, 12.36°E
28 Oct.–5 Nov. 2014	61.5	90.5	60.41°N, 15.64°E	57.82°N, 27.47°W

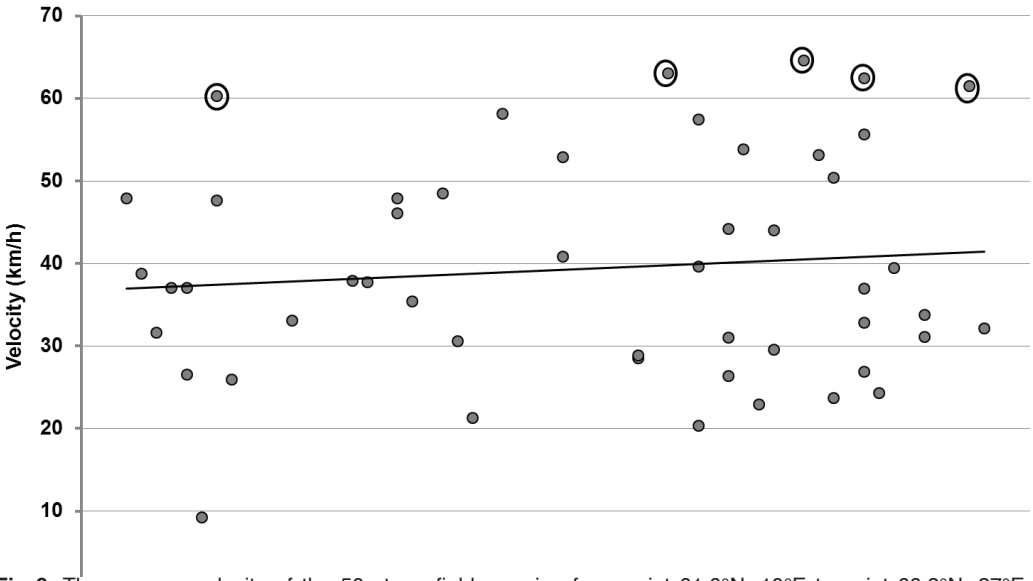

Fig 9. The average velocity of the 50 storm fields moving from point 61.6°N, 10°E to point 66.2°N, 27°E from 1958–2016. The big circles show storm fields with a velocity > 60 km h^{-1}.

We have chosen five storm fields that fit the following two criteria: the trajectory of which corresponds to the desired parameters of the model and has a velocity close to the critical value of 65 km h^{-1}, as concluded in the previous section (Table 5, Fig. 9). From Table 5, the majority of the storm fields moving along the dangerous trajectory in the area of expected maximum deepening (Fig. 3), reached a maximum velocity of up to 93 km h^{-1}. In general, they move very quickly along the whole trajectory from 10°E to 27°E, taking 24–30 hours. Estimated for the period from 1958 to 2016, the probability of a storm field passing along the trajectory from the location, 61.6°N, 10°E to the location, 66.2°N, 27°E with an average velocity exceeding 60 km h^{-1}, is established as 5/59 = 0.085 cases $year^{-1}$ or once in 11.8 years.

Of the five selected storm fields, only one (23 Sep. 2003) has a maximum depression in the specified area (P_{min} in the center of the storm field is 97 350 Pa, the Laplacian of pressure is 21.8 mPa km^{-2}), the others reach the maximum pressure low earlier. If only this storm field is taken into account, then the probability of storm fields passing along the most dangerous trajectory with the most dangerous velocity and the most dangerous point of maximum deepening is 1/59 = 0.017 cases $year^{-1}$.

Taking into account that the probability of a storm field with a maximum Laplacian of pressure in 59 mPa km^{-2} being formed over northwestern Europe is 0.001, we multiply this probability with the probability of a storm field passing along the most dangerous trajectory. We find that the probability of the calculated increase of water level in Hanhikivi to +223 cm to be 2.10^{-5} $year^{-1}$ or 0.002%.

We present the probability curves of the annual maximum level in Hanhikivi obtained by the Gumbel statistical and deterministic modeling methods (Fig. 4, curve 1 and curve 2, respectively). To construct curve 1, we used the observational data in Raahe and the relation of the water level in Raahe and Hanhikivi to extrapolate the curve. When constructing curve 2, we applied the Gumbel method to the same data and took into account the value obtained with the model and its probability (223 cm, 0.002%).

We applied the same methods to determinate the minimum sea level in Hanhikivi (results not shown). From the numerical experiments, we find that the minimum water level in Hanhikivi occurs when the extreme storm field moves from south to north with a velocity near

30 km h^{-1} along 23°E and its pressure is minimal at latitude 62.5°N (resulting extreme water level is –290 cm) or in the case of a stationary storm field with its center at 23°E, 62.5°N (resulting extreme water level is –280 cm). We find that the minimum water level extreme in Hanhikivi with a probability of 0.01% to be –251 cm.

Dvornikov *et al.* (2017) reported the stationary wind field and without taking into account atmospheric pressure, that it is practically the same maximum water level of 249 cm obtained for Hanhikivi with a probability of 0.01%, but the minimum water level reported (–151 cm) was quite different from our result.

Summary

The following conclusions can be drawn from our study in which both statistical and numerical modeling methods are applied:

1) The results of the mathematical modeling show that the maximum water level rise in Hanhikivi occurs when an extreme storm field moves in the ENE direction from the position, 61.6°N, 10°E to MP position, 66.2°N, 27°E with a velocity of 65 km h^{-1}.
2) Based on the results of mathematical modeling, the minimum water level in Hanhikivi occurs when an extreme storm field moves from south to north along 23°E with small velocity and its pressure is minimal at the latitude 62.5°N, or in the presence of a stationary storm field with its center at 23°E, 62.5°N.
3) The mathematical modeling resulted in a maximum level in Hanhikivi equal to 205 cm for 0.01% probability, the minimum level found is –251 cm.
4) For the design of the Hanhikivi Nuclear Power Plant, the most critical values obtained with statistical and deterministic methods should be used. For a probability of 0.01% (return period 10^4 years), the maximum value is +252 cm and the minimum value is –251 cm.

One of the ways to further improve the accuracy of simulating moving low pressure systems and water level oscillations induced by them is by obtaining a more detailed description of cold fronts. For example, a jump in air pressure at a cold front moving at a speed close to the long wave speed in the sea below may lead to the generation of the so-called, "meteotsunamis" (Pellikka *et al.* 2014), which are additional high frequency water level oscillations.

Acknowledgements: We thank Izabella Goldberg, Patrick Michael Platner and Herman Gerritsen for reading the article and useful comments.

References

Averkiev A.S. & Klevannyy K.A. 2009. Calculation of extreme water levels in the eastern part of the Gulf of Finland. *Russian Meteorology and Hydrology* 34 (11): 741–747.

Averkiev A.S.& Klevannyy K.A. 2010. A case study of the impact of cyclonic trajectories on sea-level extremes in the Gulf of Finland. *Continental Shelf Research* 30(6): 707–714.

Apukhtin A.A., Bessan G.N., Gordeeva S.M., Klevannaya M.K. & Klevannyy K.A. 2017. Simulation of the probable maximum flood in the area of the Leningrad nuclear power plant with account of wind waves. *Russian Meteorology and Hydrology* 42 (2): 67–77.

Blackman D.L. & Graff L.K. 1978. The analyses of annual extreme sea levels at certain ports in southern England. *Proc. Inst. Civ. Eng.* 2(65): 339–357.

Barbosa S.M. 2008. Quantile trends in Baltic Sea level. *Geophysical Research Letters.* 35: 1–6.

Bretschneider C.L. 1972. A non-dimensional stationary hurricane wave model. *Proceedings of the Offshore Technology Conference.* Houston, Texas 1: 51–68.

Dvornikov A.Y., Martyanov S.D., Ryabchenko V.A., Eremina T.R., Isaev A.V. & Sein D.V. 2017. Assessment of extreme hydrological conditions in the Bothnian Bay, Baltic Sea, and the impact of the nuclear power plant Hanhikivi-1 on the local thermal regime. *Earth System Dynamics.* 8: 265–282.

German V. Kh. & Levikov S.P. [Герман В.Х. & Левиков С.П.] 1988. *Probability analysis and modeling of sea level oscillations.* Leningrad, Gidrometeoizdat [in Russian].

Helander J. 2017. Identification and Analysis of External Event Combinations for Hanhikivi 1 PRA. *Nuclear Engineering and Technology.* 49 (2): 380–386.

International Atomic Energy Agency. 2011. *Meteorological and hydrological hazards in site evaluation for nuclear installations.* Specific safety guide. IAEA safety standards series SSG-18.

Jarosz E., Mitchell D.A., Wang D.W. & Teague W.J. 2007. Bottom-up determination of air-sea momentum

exchange under a major tropical cyclone. *Science* 315: 1707–1709.

Johansson M., Boman H., Kahma K. & Launiainen J. 2001. Trends in sea level variability in the Baltic Sea. *Boreal Environmental Research* 6: 159–179.

Johnson N. L., Kotz S. & Balakrishnan N. 1995. *Continuous univariate distributions: Vol. 2*. Second Edition. NY: Wiley.

Klevannyy K.A., Matveyev G.V. & Voltzinger N.E. 1994. An integrated modelling system for coastal area dynamics. *Int. J. Numer. Meth.Fluids* 19: 181–206.

Klevannyy K.A. & Mostamandy S.M.W. 2009. Quality of water level forecasts in St.Petersburg with four times per day model runs. *Proceedings of International Workshop Flood Vulnerability and Flood Protection in Tidal and Non-Tidal Regimes: North and Baltic Seas*. Deltares, Delft, The Netherlands. 17–18.

Klevannyy K.A. & Smirnova E.V. [Клеванный К.А. & Смирнова Е.В.] 2009. [Applications of CARDINAL software package]. *Zhurnal Universiteta vodnych communikatzii* 1: 153–162. [In Russian].

Kouroutzoglou J., Flocas H.A., Simmonds I., Keay K. & Hatzaki M. 2011. Assessing characteristics of Mediterranean explosive cyclones for different data resolution. *Theor. Appl.Climatol*. 105: 263–275.

Leppäranta M. & Myrberg K. 2009. *Physical Oceanography of the Baltic Sea*. Chichester, UK, Praxis publishing Ltd.

Okubo A. & Ozmidov R. V. 1970. An empirical relationship between the horizontal eddy diffusivity in the ocean and the scale of the phenomenon. *Izv. Atmosph. Ocean. Phys.* 6. 534–536.

Oosterbaan R.J. 2019. Software for generalized and composite probability distributions. *International Journal of Mathematical and Computational Methods* 4: 1–9.

Makin V.K. 2005. A note on drag of the sea surface at hurricane winds. *Boundary layer meteorology* 115: 169–176.

Miyazaki M., Ueno T. & Unoki S. 1962. Theoretical investigations of storm surges along the Japanese coast. *Oceanogr. Mag.* 13: 103–117.

Pellikka H., Rauhala J., Kahma K., Stipa T., Boman H. & Kangas A. 2014. Recent observations of meteotsunamis on the Finnish coast. *Natural Hazards* 74 (1): 197–215.

PSMSL 2019. *Permanent Service for Mean Sea Level,* available at: https://www.psmsl.org/data/obtaining/stations/240.php.

Serreze M.C. 2016. *Northern hemisphere cyclone locations and characteristics from NCEP/NCAR Reanalysis Data*. Boulder, Colorado USA: National Snow and Ice Data Center, available at http://nsidc.org/data/nsidc-0423.html.

Sikan A.V. [Сикан А.В.] 2007. [*Methods of statistical processing of hydrometeorological information*]. Rossiiskii Gosudarstvennyi Gidrometeorologicheskii Universitet, 7, St. Petersburg. [In Russian].

Soomere T., Behrens A., Tuomi L. & Nielsen J.W. 2008. Wave conditions in the Baltic Proper and in the Gulf of Finland during windstorm Gudrun. Nat. *Hazards Earth Syst. Sci.* 8: 37–46.

Sorkina A.I. [Соркина А.И.] 1958. [*Mapping of wind fields for the seas and oceans*]. Trudy Gosudarstvennogo Okeanograficheskogo Instituta, 44, Moscow. [In Russian].

Suursaar Ü., Kullas T., Otsmann M., Saaremäe I., Kuik, J., Merilain M. 2006. Cyclone Gudrun in January 2005 and modeling its hydrodynamic consequences in the Estonian coastal waters. *Boreal Environmental Research* 11: 143–159.

Thompson J.F., Warsi Z.U.A. & Mastin C.W. 1985. *Numerical Grid Generation. Foundation and Application*. North-Holland Publ.

Vyazilova N.A. & Vyazilova A.E. 2014. Storm cyclones in the North Atlantic. *Russian Meteorology and Hydrology* 39 (6): 371–377.

Wolski T., Wiśniewski B., Giza A., Kowalewska-Kalkowska H., Boman H., Grabbi-Kaiv S., Hammarklint T., Holfort J. & Lydeikaite Ź. 2014. Extreme sea levels at selected stations on the Baltic Sea coast. *Oceanologia* 56(2): 259–290.